2013 IEEE/RSJ International Conference on
Intelligent Robots and Systems (IROS)
November 3-7, 2013. Tokyo, Japan

Quadrupedal Bounding with Spring-damper Body Joint

Ryuta Yamasaki, Yuichi Ambe, Shinya Aoi and Fumitoshi Matsuno

***Abstract*— Stable locomotion indicates a stable limit cycle generated in the dynamic system. Although quadrupedal bound gait models have been investigated, there is no research which shows the generation of limit cycle and its dynamic properties. In the present study, we analyze a quadrupedal bound gait model which goes down slope and has back and front bodies with spring-damper joint between the bodies. We found the periodic bound gait which achieves a stable limit cycle and convergence property against perturbations.**

I. Introduction

Legged animals show diverse locomotor behaviors to adapt to various environments, where they show not only static locomotion but also dynamic locomotion. For example, they run and jump on cliffs which have limited footholds, and they jump over obstacles while running on grassland. Based on their locomotion, various legged robots have been developed [1], [2], [3], [4]. However, no robot can realize highly dynamic locomotion as legged animals.

Legged animals utilization of flexion and extension of their bodies suggests the importance of these functions. Although previous legged robots often had one rigid body, Refs. [5] and [6] used more than one rigid body and Ref. [7] used a wobbling mass body. In this study, we focus on the pitch movement of flexion and extension of the body in the sagittal plane during a bound gait, where the left and right legs simultaneously kick the ground. We construct a quadrupedal bound model in the sagittal plane which has two rigid bodies with spring-damper joint. Using this, we conduct computer simulations to investigate its dynamic properties.

II. Background

A. Researches of the bound gait

According to Full and Koditscheck [8], "In humans, dogs, lizards, crabs, cockroaches and even centipedes, the center of mass falls to its lowest position at midstance as if compressing a virtual leg spring and rebounds during the second half of the step as if recovering stored elastic strain energy." Based on this, a Spring Loaded Inverted Pendulum (SLIP) model has been developed, which is a spring-mass system in the sagittal plane to model the locomotion of running animal. Poulakakis *et al.* [9] created a periodic bound gait using springs and rigid links based on the SLIP. They show that although the gait is neutrally stable, it can tolerate some perturbations. Recent investigations use two rigid bodies for a bound gait model with spring joint between the bodies [10], [11], [12]. In [10], the body joint was controlled by PID and vibrates as designed. In [11], the quasi passive bound gait was produced by locking the joint at the appropriate timing. In [12], the periodic bound gait was generated by using a passive and conservative system.

We can summarize the previous studies about quadrupedal bound gait as follows.

1) Ref. [9] used one rigid body model and realized a periodic bound gait which is neutrally stable.
2) Refs. [10] and [11] used two rigid bodies with a spring joint and generated the bound gait.
3) Ref. [12] used two rigid bodies with a spring joint and produced the periodic bound gait. This gait was neutrally stable. It did not achieve a limit cycle and was not asymptotically stable.

B. Purpose of this study

It is useful to apply dynamic characteristics in the locomotion of legged animals to legged robots. To clarify their features, passive dynamics is important. From such a point of view, Refs. [9] and [12] generated a periodic bound gait, as described above. However, due to their limitation of conservative system, asymptotic stability and limit cycle have not been discussed. Therefore, in this paper, we construct a quadrupedal bounding gait model, which has two rigid bodies with a spring-damper joint and goes down a slope. In contrast to their models, our model has a damping at the body joint, which allows the model to produce asymptotically stable locomotion. The purpose of this paper is to find a stable periodic bound gait of our planar model and to analyze the features of the periodic gait.

III. Simulation

A. Model

In this paper, we use a planar model (Fig. 1) based on the model of Poulakakis *et al.* [9], where we added a spring-damper body joint. We refered to [14] to build a dynamics simulator. Tables I and II show the variables and parameters of the model. The body consists of two rigid bodies, which are connected by a spring-damper joint to simulate the flexibility of the body. Mass of back and front bodies are m_1 and m_2, their moments of inertia around the center of mass are I_1 and I_2. Spring and damper coefficients of the body joint are k_c and c_c. The rotational spring is at the equilibrium position where the front and back bodies are parallel ($\theta_2 = 0$). We assume that back and front legs have

R. Yamasaki, Y. Ambe and F. Matsuno are with the Department of Mechanical Engineering and Science, Graduate School of Engineering, Kyoto University, Kyotodaigakukatsura, Nishikyo-ku, Kyoto, 615-8540, Japan yamasaki.ryuta.43n@st.kyoto-u.ac.jp amby.yu@gmail.com matsuno@me.kyoto-u.ac.jp

S. Aoi is with the Department of Aeronautics and Astronautics, Graduate School of Engineering, Kyoto University, Kyotodaigakukatsura, Nishikyo, Kyoto, 615-8540, Japan shinya_aoi@kuaero.kyoto-u.ac.jp

978-1-4673-6357-0/13/$31.00

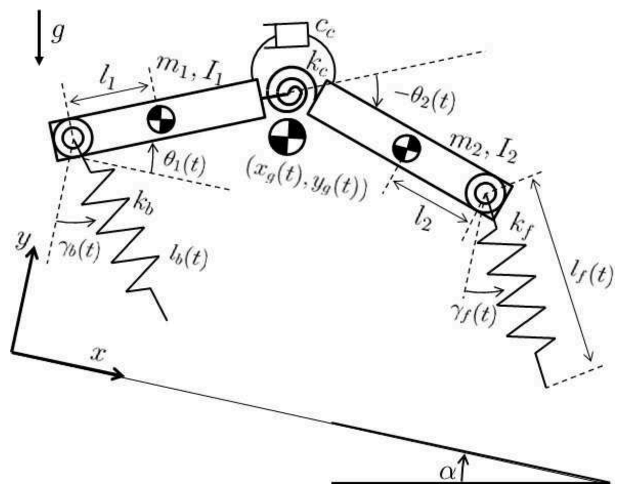

Fig. 1. Quadrupedal bounding gait model with articulated body and a spring-damper body joint

TABLE I
DEFINITION OF PARAMETER

cartesian coordinates of the robot COM	$(x_g(t), y_g(t))$
pitch angle of the back body	$\theta_1(t)$
relative angle of the front body from back body	$\theta_2(t)$
length of back, front leg	$l_b(t)$, $l_f(t)$
angle of back, front leg	$\gamma_b(t)$, $\gamma_f(t)$
gravity acceleration	g
slope angle	α
mass of back, front body	m_1, m_2
moment of inertia about COM of back, front body	I_1, I_2
length of back, front body	$2l_1$, $2l_2$
nominal length of back, front leg	$\bar{l}_b$, $\bar{l}_f$
spring stiffness of back, front leg	k_b, k_f
rotational spring stiffness (between bodies)	k_c
damping coefficient of body joint	c_c
mass of back, front leg	0

no mass, and their stiffness are k_b and k_f, respectively. The leg tip becomes a frictionless pin joint when it is on the ground. In other words, the tip does not move when it is on the ground and the leg rotates freely. The leg is attached to the body by a frictionless pin joint. This model goes down a slope whose angle is α.

TABLE II
MODEL PARAMETERS

Parameter	Value	
g	9.8	m/s^2
m_1, m_2	10.4	kg
$2l_1$, $2l_2$	0.55	m
$\bar{l}_b$, $\bar{l}_f$	0.32	m
I_1, I_2	0.64	kg m^2
h_b, h_f	0.33	m

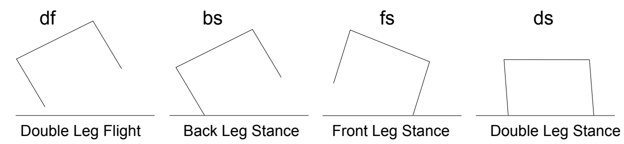

Fig. 2. Four stance conditions

B. Bound gait

In this paper, two types of bound gaits are considered. One gait contains a phase where the front and back legs are simultaneously on the ground. The other gait doesn't have such a phase. Details of the bound gaits and governing equations of motion are shown below:

1) Classification of stance condition of bound gait: There are four types of stance conditions as shown in Fig. 2. When the back and front legs are floating, we named this condition as df (Double Leg Flight). When only back leg is on the ground, we named this condition as bs (Back Leg Stance). When only front leg is on the ground, we named this condition as fs (Front Leg Stance). When the back and front legs are on the ground, we named this condition as ds (Double Leg Stance).

2) Conditions of switching the stance phase: The $y-$coordinate of the center of mass of the back body, y_1, is given by

$$y_1 = y_g - \frac{m_2}{m_1+m_2}\left(l_1 \sin\theta_1 + l_2 \sin(\theta_1+\theta_2)\right) \qquad (1)$$

We denote γ_b^{td} and γ_f^{td} for the touch down angles of the back and front legs. Conditions of switching the four stance conditions (df, bs, fs and ds) are shown below:

1) Double Leg Flight to Back Leg Stance (df $\Rightarrow$ bs)
   - $y_1 - l_1 \sin\theta_1 - \bar{l}_b \cos\gamma_b^{td} = 0$
2) Back Leg Stance to Double Leg Flight (bs$\Rightarrow$df)
   - $l_b - \bar{l}_b = 0$
3) Double Leg Flight to Front Leg Stance (df$\Rightarrow$fs)
   - $y_1 + l_1 \sin\theta_1 + 2l_2 \sin(\theta_1+\theta_2) - \bar{l}_f \cos\gamma_f^{td} = 0$
4) Front Leg Stance to Double Leg Flight (fs$\Rightarrow$df)
   - $l_f - \bar{l}_f = 0$
5) Back Leg Stance to Double Leg Stance (bs$\Rightarrow$ds)
   - $y_1 + l_1 \sin\theta_1 + 2l_2 \sin(\theta_1+\theta_2) - \bar{l}_f \cos\gamma_f^{td} = 0$
6) Double Leg Stance to Front Leg Stance (ds$\Rightarrow$fs)
   - $l_b - \bar{l}_b = 0$

3) Classification of bound gait: Bound gait of our model is classified into two types. One does not have Double Leg Stance (ds) and the stance conditions are changed through 1$\Rightarrow$2$\Rightarrow$3$\Rightarrow$4$\Rightarrow$1... The other has Double Leg Stance (ds) (1$\Rightarrow$5$\Rightarrow$6$\Rightarrow$4$\Rightarrow$1...).

C. Equations of motion

Eight variables $[x_g\ y_g\ \theta_1\ \theta_2\ \gamma_b\ l_b\ \gamma_f\ l_f]$ determine the state of this model. However, when the back leg is floating, γ_b and l_b have no effect on the motion, and when the front leg is floating γ_f and l_f have no effect on the motion because of the assumption that legs have no mass. When the back leg is on the ground, γ_b and l_b are described by four variables x_g, y_g, θ_1 and θ_2. When the front leg is on the ground, γ_f and l_f are described by four variables x_g, y_g, θ_1 and θ_2 because of the assumption that leg tip is a frictionless pin joint. Therefore, we can describe equations of motion by four variables: $\boldsymbol{q} = [x_g \ y_g \ \theta_1 \ \theta_2]^T$. We define V_σ as potential energy (σ = df, bs, fs, ds), T as kinetic energy, and Δ as dissipation function, which are given by

$$V_\sigma = (m_1 y_1 + m_2 y_2)\, g \cos\alpha - (m_1 x_1 + m_2 x_2)\, g \sin\alpha \quad (2)$$
$$+\frac{1}{2}\{k_c\left(\theta_2 - \bar{\theta}_2\right)^2 + k_b\left(l_b - \bar{l}_b\right)^2 + k_f\left(l_f - \bar{l}_f\right)^2\}$$

$$T = \frac{1}{2}\{m_1\left(\dot{x}_1^2 + \dot{y}_1^2\right) + m_2\left(\dot{x}_2^2 + \dot{y}_2^2\right) + I_1\dot{\theta}_1^2 + I_2\left(\dot{\theta}_1 + \dot{\theta}_2\right)^2\} \quad (3)$$

$$\Delta = \frac{1}{2} c_c \dot{\theta}_2^2 \quad (4)$$

where (x_1, y_1) and (x_2, y_2) are the coordinates of center of mass of the back and front bodies and are given by

$$x_1 = x_g - \frac{m_2}{m_1 + m_2}\left(l_1\cos\theta_1 + l_2\cos(\theta_1 + \theta_2)\right) \quad (5)$$
$$y_1 = y_g - \frac{m_2}{m_1 + m_2}\left(l_1\sin\theta_1 + l_2\sin(\theta_1 + \theta_2)\right) \quad (6)$$
$$x_2 = x_g + \frac{m_1}{m_1 + m_2}\left(l_1\cos\theta_1 + l_2\cos(\theta_1 + \theta_2)\right) \quad (7)$$
$$y_2 = y_g + \frac{m_1}{m_1 + m_2}\left(l_1\sin\theta_1 + l_2\sin(\theta_1 + \theta_2)\right) \quad (8)$$

l_b and l_f depend on the stance condition as follows.

- Double leg flight (σ =df)
$$l_b = \bar{l}_b, \qquad l_f = \bar{l}_f \quad (9)$$
- Back leg stance (σ =bs)
$$l_b = \sqrt{A^2 + C^2}, \qquad l_f = \bar{l}_f \quad (10)$$
- Front leg stance (σ =fs)
$$l_b = \bar{l}_b, \qquad l_f = \sqrt{B^2 + D^2} \quad (11)$$
- Double leg stance (σ =ds)
$$l_b = \sqrt{A^2 + C^2}, \qquad l_f = \sqrt{B^2 + D^2} \quad (12)$$

where,

$$A = x_b^{toe} + l_1\cos\theta_1 - x_1, \quad B = x_f^{toe} - l_2\cos(\theta_1 + \theta_2) - x_2 \quad (13)$$

$$C = y_1 - l_1\sin\theta_1, \qquad D = y_2 + l_2\sin(\theta_1 + \theta_2). \quad (14)$$

x_b^{toe} and x_f^{toe} are x coordinates of back and front toe on the ground.

From Lagrangian equation, the equations of motion are given by

$$\frac{d}{dt}\left(\frac{\partial L_\sigma}{\partial \dot{\boldsymbol{q}}}\right) - \frac{\partial L_\sigma}{\partial \boldsymbol{q}} = -\frac{\partial \Delta}{\partial \dot{\boldsymbol{q}}}, \quad (15)$$

where

$$L_\sigma = T - V_\sigma. \quad (16)$$

The four equations of motion obtained by equation (15) are switched according to the conditions in I-B.2 to conduct dynamics simulation.

D. Searching for periodic bound gait with body joint oscillation

1) Periodic bound gait: In a periodic bound gait, one state and the state after one cycle are identical. In this section, we solve a discrete problem to generate a periodic stable bound gait. We define Poincaré section S_{apex} when the center of mass of the robot reaches the highest point at the Double Leg Flight (df) condition.

$$S_{apex} = \{\boldsymbol{z} \in R^6 \mid \dot{y}_g = 0, \sigma = df\} \quad (17)$$

Leg angles γ_b and γ_f move instantly when the leg lifts off the ground. Therefore, γ_b and γ_f have always the same value on the Poincaré section. Therefore, we define variables on S_{apex} as $\boldsymbol{z} = [y_g \ \theta_1 \ \theta_2 \ \dot{x}_g \ \dot{\theta}_1 \ \dot{\theta}_2]^T$ to solve the discrete problem. We define Poincaré map $\boldsymbol{P}$ as mapping $\boldsymbol{z}_0$ to $\boldsymbol{z}_1$, which is given by

$$\boldsymbol{z}_1 = \boldsymbol{P}\ (\boldsymbol{z}_0) \quad (18)$$

The condition for a periodic bound gait is $\boldsymbol{z}_0^* - \boldsymbol{P}\ (\boldsymbol{z}_0^*) = 0$. So, we find a fixed point $\boldsymbol{z}_0^*$ on the Poincaré section to produce a periodic bound gait.

2) Stability of periodic bound gait: We estimate the stability of a periodic bound gait by the maximum eigenvalue of Jacobian matrix of Poincaré map [13]. We denote perturbation from $\boldsymbol{z}^*$ by $\Delta\boldsymbol{z}$.

$$\boldsymbol{z}^* + \Delta\boldsymbol{z}_1 = \boldsymbol{P}(\boldsymbol{z}^* + \Delta\boldsymbol{z}_0) \quad (19)$$
$$= \boldsymbol{P}(\boldsymbol{z}^*) + [\nabla\boldsymbol{P}(\boldsymbol{z}^*)]\Delta\boldsymbol{z}_0 + O\left(\|\Delta\boldsymbol{z}_0\|^2\right) \quad (20)$$

where $\nabla\boldsymbol{P}(\boldsymbol{z}^*)$ is a 6×6 matrix called the linearized Poincaré map at $\boldsymbol{z}^*$. Since $\boldsymbol{z}^* = \boldsymbol{P}(\boldsymbol{z}^*)$, we get

$$\Delta\boldsymbol{z}_1 = [\nabla\boldsymbol{P}(\boldsymbol{z}^*)]\Delta\boldsymbol{z}_0 \quad (21)$$

We denote λ_j $(j = 1, \ldots, 6)$ for eigenvalues of $\nabla\boldsymbol{P}(\boldsymbol{z}^*)$. If and only if $\mid \lambda_j \mid < 1$ for all j, periodic bound gait is asymptotically stable. $\nabla\boldsymbol{P}(\boldsymbol{z}^*)$ is approximated by

$$\nabla\boldsymbol{P}(\boldsymbol{z}^*) = \frac{\partial\boldsymbol{P}}{\partial\boldsymbol{z}} = \left[\frac{\partial\boldsymbol{P}}{\partial y_g}\ \frac{\partial\boldsymbol{P}}{\partial\theta_1}\ \frac{\partial\boldsymbol{P}}{\partial\theta_2}\ \frac{\partial\boldsymbol{P}}{\partial\dot{x}_g}\ \frac{\partial\boldsymbol{P}}{\partial\dot{\theta}_1}\ \frac{\partial\boldsymbol{P}}{\partial\dot{\theta}_2}\right] \quad (22)$$

where

$$\frac{\partial\boldsymbol{P}}{\partial z_i} = \frac{\boldsymbol{P}(z_1^*, \ldots, z_i^* + dz, \ldots, z_6^*) - \boldsymbol{P}(z_1^*, \ldots, z_i^* - dz, \ldots, z_6^*)}{2dz} \quad (23)$$

In this paper, we used $dz = 10^{-6}$.

3) Damping ratio: We determine the damping ratio of the body joint based on the equation of motion of the oscillation of the body joint between two rigid bodies, which is given by

$$\ddot{\theta}_2 + 2\zeta\omega_n\dot{\theta}_2 + \omega_n^2\theta_2 = 0 \tag{24}$$

where,

$$\omega_n = \sqrt{\frac{k(I_1^{'} + I_2^{'})}{I_1^{'}I_2^{'}}}, \qquad \zeta = \frac{c_c}{2}\sqrt{\frac{I_1^{'} + I_2^{'}}{I_1^{'}I_2^{'}k_c}} \tag{25}$$

$$I_1^{'} = m_1 l_1^2 + I_1, \qquad I_2^{'} = m_2 l_2^2 + I_2 \tag{26}$$

We determine the damping ratio ζ from (25).

4) Method of searching periodic bound gait: We used the following process to find the condition $[k_c,\ k_b,\ k_f,\ \gamma_b,\ \gamma_f,\ \boldsymbol{z}^*]$ of a fixed point on the Poincaré section S_{apex} for small rotational spring stiffness k_c. This process starts from a certain initial condition $[k_c^i,\ k_b^i,\ k_f^i,\ \gamma_b^i,\ \gamma_f^i,\ \boldsymbol{z}_0^i]$ and we repeat this process to find sets of fixed points depending on k_c.

- A Use the condition of previous fixed point as an initial parameter.
- B Decrease the rotational spring stiffness k_c.
- C Find a slope angle α to produce a periodic bound gait (see details in I-D.5). Specifically, using an updated slope angle, we simulate 100 steps and evaluate the error of each state variable between $\boldsymbol{z}_{99}$ and $\boldsymbol{z}_{100}$. If the error is less than 10^{-5}, the state variable $\boldsymbol{z}_{100}$ and the other variables are regarded to be the condition of fixed point. $\rightarrow$ back to B
- D Otherwise, update an initial state $\boldsymbol{z}_0$ by Newton-Raphson method $\rightarrow$ back to C
- E If any fixed point isn't found after updating 100 times by Newton-Raphson method, the touch down angle γ_b^{td} or γ_f^{td} is changed by ± 0.5 deg at a time. $\rightarrow$ back to C
- F If any fixed point isn't found after changing the touch down angle ± 4 deg, a set of leg stiffness $(k_b,\ k_f)$ is changed by ± 100 N/m each at a time. $\rightarrow$ back to C

5) Determination of slope angle: In the process C, we determined the slope angle to balance total energy by the following method: we set initial slope angle as α_0, then simulate 100 steps. We defined the energy error between the initial state of 100th step and the final state as ΔE_0. We set the first updated slope angle as α_1, then simulate 100 steps, and define the energy error between the initial state of 100th step and the final step as ΔE_1. After that, we changed the slope angle α_k at k th step ($k \geq 2$) based on the energy errors by

$$\alpha_k = \alpha_{k-2} - \Delta E_{k-2}\left(\frac{\alpha_{k-1} - \alpha_{k-2}}{\Delta E_{k-1} - \Delta E_{k-2}}\right) \tag{27}$$

IV. Result

A. Periodic bound gait

First, based on the periodic bound gait of one rigid body model [9], we produced a periodic bound gait of our model, where the body joint doesn't vibrate using a large rotational spring stiffness. Then, we changed the periodic gait by decreasing the spring stiffness step by step using the process of Section I-D.4.

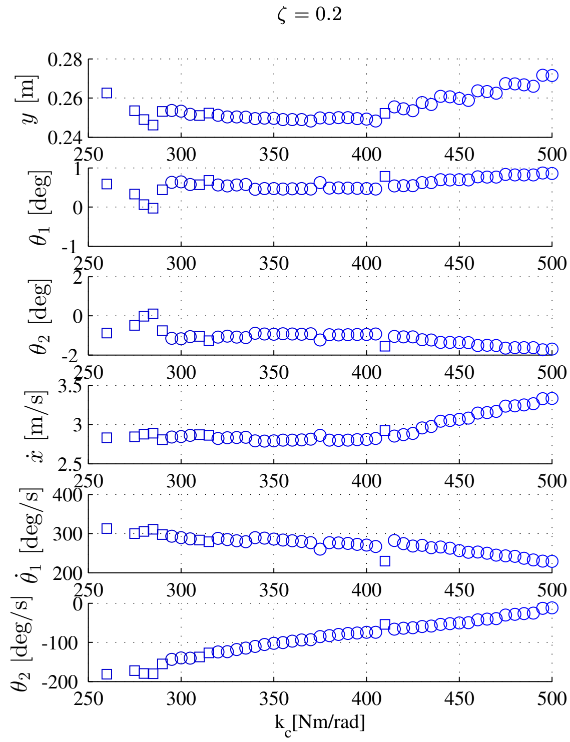

Fig. 3. Fixed points of state variables on the Poincaré section for various spring stiffness with $\zeta = 0.2$

Fig. 3 shows the state variables of the periodic bound gait on the Poincaré section using $\zeta = 0.2$. White cicle ○ does not have Double Leg Stance (ds), whereas white square □ has Double Leg Stance (ds). Fig. 4 shows the maximum eigenvalue of the linearized Poincaré map about each fixed point (namely, maximum value of eigenvalues of $\nabla\boldsymbol{P}(\boldsymbol{z}^*)$ explained in I-D.2, we define this as e_{max}), touch down angle, leg spring stiffness, and slope angle. In the figure of the touch down angle γ_b^{td} and γ_f^{td}, white circle ○ and white square □ are for the back leg touch down angle, while black circle ● and black square ■ are for the front leg touch down angle.

B. Periodic bound gait with body vibration

We found a periodic bound gait whose body vibration had an amplitude of about 5 deg by using $k_c = 295$, $\zeta = 0.2$, $\alpha = 1.93$, $\gamma_b = 46.7$, $\gamma_f = 44.6$ and $k_b = k_f = 2420$, where $\boldsymbol{z}^* = [y_g^*\quad \theta_1^*\quad \theta_2^*\quad \dot{x}_g^*\quad \dot{\theta}_1^*\quad \dot{\theta}_2^*] = [0.2536\,\mathrm{m}\quad 0.6303\,\mathrm{deg}\quad -1.152\,\mathrm{deg}\quad 2.840\,\mathrm{m/s}\quad 293.2\,\mathrm{deg/s}\quad -143.7\,\mathrm{deg/s}]$. In this section, we focus on this periodic bound gait.

1) Periodic solution of each state valuable: Fig. 5 shows the periodic solution of each state variables. Vertical dotted lines show the time when the stance condition was changed. The lines mean df$\rightarrow$bs, bs$\rightarrow$df, df$\rightarrow$fs, fs$\rightarrow$df and $\dot{y}_g = 0$ in

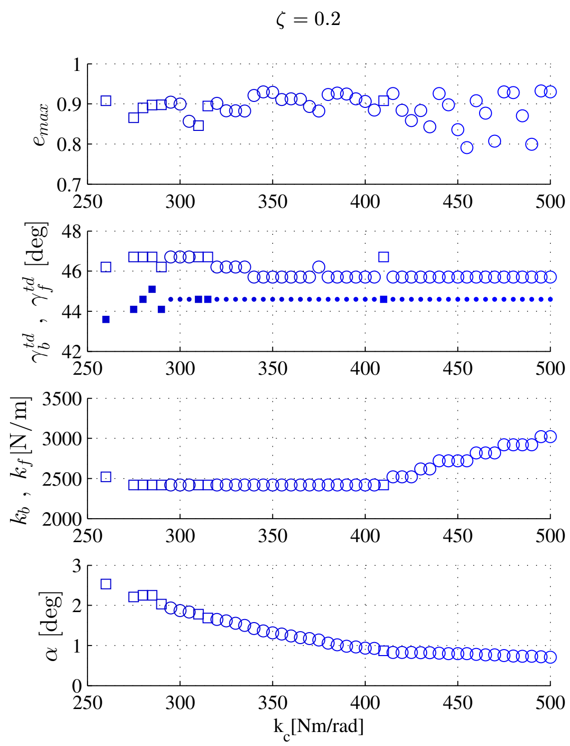

Fig. 4. Parameter values of periodic bound gait for spring stiffness k_c with $\zeta = 0.2$

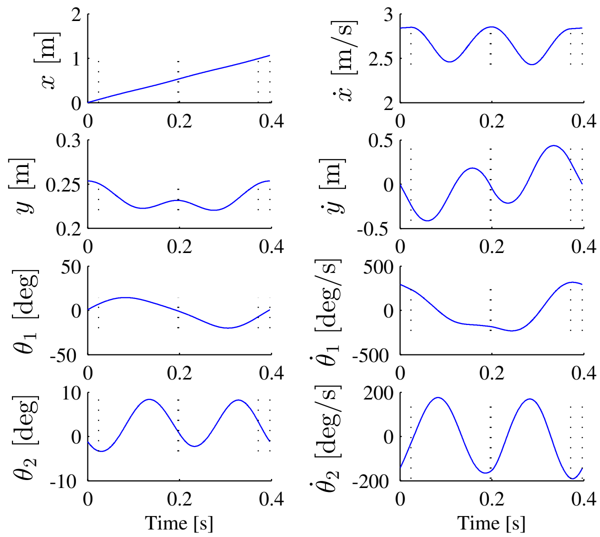

Fig. 5. Periodic solution of bound gait with $k_c = 295$ and $\zeta = 0.2$

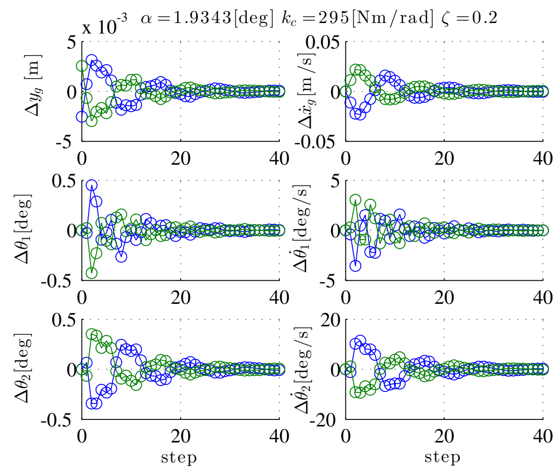

Fig. 6. Convergence of state variables against perturbation of y_g with $\alpha = 1.9343$, $k_c = 295$ and $\zeta = 0.2$

order. Because bs→df and df→fs occurred in a short interval (0.002 s), these two lines are difficult to be distinguished. θ_2 shows that this periodic bound gait has two body oscillations during one gait cycle. Body bent after the back leg touched down, and bent again after the front leg touched down. We did not find a periodic solution with single body oscillation during one step in this simulation.

2) Existence of limit cycle: Maximum eigenvalue of linearized Poincaré map was close to 1 at a large rotational spring stiffness k_c, but it became smaller to be around 0.9 when the rotational spring stiffness k_c decreased to some extent. Therefore, this periodic bound gait is expected to be asymptotically stable. This stability is examined by perturbing each state variable on the Poincaré section.

Fig. 6 shows the time evolution of each state variable when y_g of the fixed point was perturbed $\pm 1\%$ from y_g^* while k_c, α, and other parameters were not changed. Δz indicates the disturbance from the fixed point of z. The state variables converged to their fixed point in about 40 steps. When other variables $\dot{x}$, θ_1, θ_2, $\dot{\theta}_1$ and $\dot{\theta}_2$ were perturbed, the state variables also converged to the original fixed point. From these results, we can conclude that this system has a stable limit cycle.

3) Properties of periodic gait with body vibration: To investigate the properties of the periodic gait with body oscillation, we changed the slope angle α or k_c and found periodic gaits by

1) Increase or decrease α or k_c
2) Estimate convergence after 100 steps. Specifically, if the error between the initial state of 100th step and the final state of this step is less than 10^{-5} for all state variables, we decide the state variables converged to a fixed point.
3) Examine the maximum eigenvalue of the fixed point.

Fig. 7 shows the maximum eigenvalue when we changed the slope angle α while the other parameters are fixed. This resulted in $\boldsymbol{z}^* = [y_g^* \quad \theta_1^* \quad \theta_2^* \quad \dot{x}_g^* \quad \dot{\theta}_1^* \quad \dot{\theta}_2^*] = [0.2536\,\text{m} \quad 0.6303\,\text{deg} \quad -1.152\,\text{deg} \quad 2.840\,\text{m/s} \quad 293.2\,\text{deg/s} \quad -143.7\,\text{deg/s}]$. Fig. 8 shows the maximum eigenvalue when we changed the spring stiffness k_c. When we did not change α or k_c ($\alpha = 1.93$, $k_c = 295$), the periodic bound gait did not have Double Leg Stance (ds) condition, as shown by blue circles ●. When we changed α or k_c, the state variables were converged to a periodic gait with Double Leg Stance (ds) condition, as shown by green squares ■. We found that this model can keep a stable bound gait in the range of 1.92

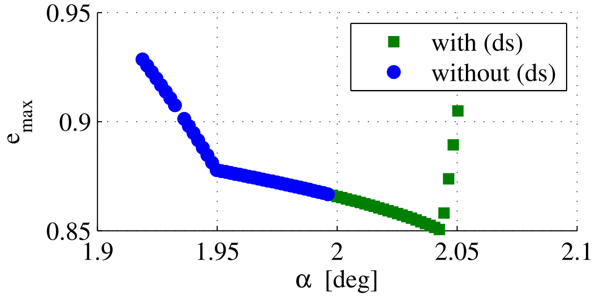

Fig. 7. Maximum eigenvalue when the slope angle α is changed

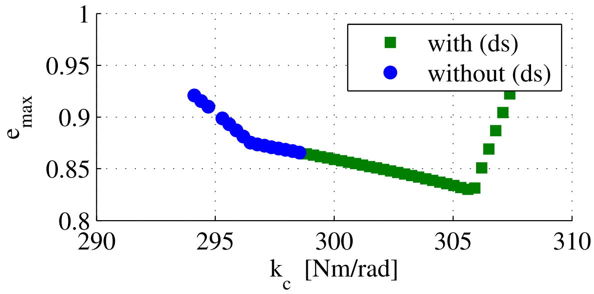

Fig. 8. Maximum eigenvalue when the rotational spring stiffness k_c is changed

- 2.05 deg for the slope angle α and 294 - 308 Nm/rad for the rotational spring stiffness k_c. If the slope angle or the rotational spring stiffness exceeds a certain value, the gait was changed from the gait without Double Leg Stance (ds) to the gait with Double Leg Stance (ds). However, in this result, the duration of Double Leg Stance (ds) was so short that the locomotion behavior did not change remarkably.

V. Conclusion

To understand natural mechanical property of bound gait we used a bound gait model with two bodies and a spring-damper joint and analyzed the dynamic properties. We got the following results.

- Periodic gaits were found for various rotational spring stiffness k_c.
- The maximum eigenvalue of linearized Poincaré map was less than one. The gait has a stable limit cycle.
- By changing slope angle α or rotational spring stiffness k_c, stability and gait pattern were changed.

For future works, we would like to find a periodic bound gait where the body joint has one oscillation in one step and analyze its effect on the gait. While we showed the system becomes unstable by changing slope angle or rotational spring stiffness, we would like to investigate stability characteristics for various parameters such as bifurcation.

References

[1] U. Saranli, "RHex: A Simple and Highly Mobile Hexapod Robot", *International Journal of Robotics Research*, Vol. 20, No. 7, pp. 616–631, 2001.

[2] Y. Fukuoka, H. Kimura, and a. H. Cohen, "Adaptive Dynamic Walking of a Quadruped Robot on Irregular Terrain Based on Biological Concepts", *International Journal of Robotics Research*, Vol. 22, No. 3-4, pp. 187–202, 2003.

[3] I. Poulakakis, "Modeling and Experiments of Untethered Quadrupedal Running with a Bounding Gait: The Scout II Robot", *International Journal of Robotics Research*, Vol. 24, No. 4, pp. 239–256, 2005.

[4] Y. Ambe and F. Matsuno, "Leg-grope-walk — Walking strategy on weak and irregular slopes for a quadruped robot by force distribution", *In Proc. IEEE/RSJ International Conference on Intelligent Robots and Systems*, pp. 1840–1845, 2012.

[5] S. Aoi, H. Sasaki, and K. Tsuchiya, "A Multilegged Modular Robot That Meanders: Investigation of Turning Maneuvers Using Its Inherent Dynamic Characteristics", *SIAM Journal on Applied Dynamical Systems*, Vol. 6, No. 2, pp. 348–377, 2007.

[6] S. Aoi, T. Yamashita, and K. Tsuchiya, "Hysteresis in the gait transition of a quadruped investigated using simple body mechanical and oscillator network models", *Physical Review. E*, Vol. 83, No. 6, pp. 061909-1–061909-12, 2011.

[7] C. D. Remy, K. W. Buffinton, and R. Siegwart, "Stability Analysis of Passive Dynamic Walking of Quadrupeds", *International Journal of Robotics Research*, Vol. 29, No. 9, pp. 1173–1185, 2009.

[8] R. J. Full and D. E. Koditschek. "Templates and anchors: neuromechanical hypotheses of legged locomotion on land", *Journal of Experimental Biology*, Vol. 202, No. 23, pp. 3325–32, 1999.

[9] I. Poulakakis, E. Papadopulos, and M. Buehler, "On the Stability of the Passive Dynamics of Quadrupedal Running with a Bounding Gait", *International Journal of Robotics Research*, Vol. 25, No. 7, pp. 669–687, 2006.

[10] U. Culha and U. Saranli. "Quadrupedal bounding with an actuated spinal joint", *In Proc. IEEE International Conference on Robotics and Automation*, pp. 1392–1397, 2011.

[11] Qi Deng, Shigang Wang, Wei Xu, Jinqiu Mo, and Qinghua Liang, "Quasi passive bounding of a quadruped model with articulated spine", *Mechanism and Machine Theory*, Vol. 52, pp. 232–242, 2012.

[12] Qu Cao and Ioannis Poulakakis, "Passive quadruped bounding with a segmented flexible torso", *In Proc. IEEE/RSJ International Conference on Intelligent Robots and Systems*, pp. 2484-2489, 2012.

[13] S. Strogatz, "Nonlinear Dynamics and Chaos: With Applications To Physics, Biology, Chemistry, and Engineering (Studies in Nonlinearity)", *Westview Press*, 2001.

[14] C. D. Remy, K. Buffinton, and R. Siegwart, "A MATLAB framework for efficient gait creation", *In Proc. IEEE/RSJ International Conference on Intelligent Robots and Systems*, pp. 190-196, 2011